Construction and Optimization of Complex Surface-Reaction Mechanisms

Preeti Aghalayam, Young K. Park, and Dionisios G. Vlachos
Dept. of Chemical Engineering, University of Massachusetts Amherst, Amherst, MA 01003

A multistep methodology for the quantitative determination of rate constants of a detailed surface-reaction mechanism is proposed. As a starting point, thermodynamically consistent, coverage-dependent activation energies and heats of reactions were derived from the application of the unity bond index−quadratic exponential potential formulation, and initial estimates of the preexpontentials were obtained from transition-state theory or available experiments. Important feature identification analysis was performed to determine key kinetic parameters for various experiments. Model responses were parameterized in terms of these important parameters by polynomials and factorial design techniques, and these parameterized responses were subsequently used in simultaneous optimization through simulated annealing against different sets of experimental data to obtain a quantitative reaction mechanism that is valid over a wide range of operating conditions. The technique was successfully applied to the development of a comprehensive reaction mechanism for H_2*/air mixtures on polycrystalline Pt.*

Introduction

Surface reaction mechanisms are at the heart of catalytic reactors that are used to manufacture a large fraction of industrial chemicals. Among various catalytic processes, partial oxidation is central to many chemical intermediates (Satterfield, 1991). The recent advances in partial oxidation of small paraffins over noble metal catalysts in short-contact time microreactors giving high selectivities and fuel-conversions [e.g., syngas production from methane (Hickman and Schmidt, 1992) and olefin production from various alkanes (Goetsch and Schmidt, 1996; Bodke et al., 1999)] have triggered considerable academic and industrial interest (Aghalayam et al., 2000). At the other end of operation, catalytic combustion has emerged as an important alternative process to flame combustion for energy production, because it provides enhanced efficiency and stability, while reducing pollutant emissions (Prasad et al., 1984; Pfefferle and Pfefferle, 1986).

Understanding and design of such processes are far from trivial, as reactor performance is the outcome of the strong interplay of heat and mass transfer with chemical kinetics under adverse conditions of short contact times, high pressures, and large gradients. Capturing the essential physics of these systems necessitates the use of detailed transport and kinetic models. While the performance of detailed transport and gas-phase chemistry schemes has been validated extensively, the surface-phase chemistry models are still underdeveloped. The existing detailed surface-reaction models are often not able to predict multiple experimental data (Aghalayam et al., 1999), and the development of mechanisms for more complex fuels is challenging.

In a recent publication, we introduced a multistep approach for determining the coverage-dependent rate constants of detailed surface-reaction mechanisms in a thermodynamically consistent manner (Park et al., 1999). This approach includes the construction of an initial trial mechanism, important feature identification of multiset experimental data, and parameter refinement. An essential part of the initial construction of the mechanism involves applying the foundations of the unity bond index−quadratic exponential potential (UBI−QEP) theory of Shustorovich and coworkers (Shustorovich and Sellers, 1998), which can provide species-coverage-dependent reaction energetics for the entire mechanism. A major advantage of this semiempirical microkinetic approach is its computational efficiency within reactor scale models that adds only a small cost to CPU requirements compared to conventional Arrhenius kinetic rate expressions.

One important step in our methodology is refinement of the kinetic parameters of the initial mechanism. This can be a time-consuming, tedious, or even impossible task to accom-

---

Correspondence concerning this article should be addressed to D. G. Vlachos at the following current address: Dept of Chemical Engineering and Center for Catalytic Science and Technology (CCST), University of Delaware, Newark, DE 19716.

plish by a computationally manual trial-and-error approach, especially for large mechanisms of hydrocarbons. In this article, we introduce for the first time a tool for the mathematically rigorous and automatic refinement of important reaction preexponentials of complex surface-reaction mechanisms. Using multiple sets of experimental data under varying conditions, factorial design and solution-mapping techniques are used to provide a means of simultaneously refining a large number of reaction parameters. Validation against additional experiments and statistical analysis is performed to determine the quality of the optimized mechanism.

In the following sections we first summarize limitations of the current approach after which we outline our generic approach. Our approach is finally demonstrated for the H_2/O_2 reaction on Pt. This reaction has been studied extensively, as it is a simple and yet an important subset of the methane reaction mechanism, and its parameters are crucial in syngas production, where H_2 is a major product (Hickman and Schmidt, 1992), and oxidative dehydrogenation of ethane to ethylene, where H_2 can be both a reactant and a product (Bodke et al., 1999).

Previous Approach of Mechanism Development and Challenges

The earlier approach of detailed surface-reaction-mechanism development consisted of laying down a set of reactions, with rate constants and sticking coefficients obtained from several independent surface science studies. Unknown kinetic parameters were subsequently fitted in order to predict a single type of experiment well (such as either ignition or selectivity data). Such mechanisms have been very useful in providing insight into the physics governing various phenomena and in particular catalyst ignition. However, there is often a lack of applicability over a wide range of operating conditions (Aghalayam et al., 1999; Park et al., 1999). Some additional challenges in developing surface-reaction mechanisms are outlined next.

Pressure and Materials Gap. Surface science experiments are conducted at ultrahigh vacuum and often on well-characterized single-crystal surfaces (Lombardo and Bell, 1991). The validity of extrapolating the kinetic parameters deduced from these experiments to predict data at high pressures, on polycrystalline or supported crystal sufaces, is an open question.

Thermodynamic Inconsistency. Overall thermodynamic consistency may be violated when activation energies of certain steps are tuned in order to fit the experimental data. Apart from violating the first law of thermodynamics, this becomes important for processes affected by heat transfer such as catalytic combustion. This problem arises because even though the heat of an elementary reaction is made equal to the difference in activation energies of the forward and backward steps, it is easy to show that the number of linearly independent heats of reactions is equal to the number of surface species. The latter is typically smaller than the number of surface reactions in a complex surface reaction network. As a result, thermodynamic consistency during optimization may not be ensured.

Adsorbate−Adsorbate Interactions. Under conditions of practical interest (e.g., high pressures), the concentrations of surface species are fairly high, leading to many adsorbate−adsorbate interactions (this aspect is associated in part with the pressure-gap mentioned earlier). An immediate consequence of these interactions is that the activation energies of the desorption steps depend on the surface coverages, a feature often accounted for in reaction mechanisms. Furthermore, all surface reactions involving these species have coverage-dependent activation energies (Shustorovich and Sellers, 1998; Park et al., 1999). Such interactions have to be incorporated in a thermodynamically consistent manner, as the potential energy surfaces (and thus the heats of reaction) are modified.

Comprehensive Set of Reaction Paths. There is a lack of experimental data on rate constants of the elementary steps of more complex fuels. Since the experimental isolation of specific paths of a complex surface-reaction mechanism is nontrivial, this limitation is a severe one, especially for fuels more complex than H_2 and CO where little information about elementary steps is available. Aside from completeness, consideration of an extensive set of reaction pathways is vital to avoid the overfitting of certain rate constants in an attempt to predict the experimental data.

New Approach to Surface-Reaction Mechanism Development

Figure 1 depicts our overall methodology. In the first step, we construct a detailed initial or trial surface-reaction mechanism, consisting of a comprehensive set of reaction pathways, with coverage-dependent activation energies and heats of reaction determined using the UBI−QEP (or bond-order conservation) theory (Shustorovich, 1990; Shustorovich and Sellers, 1998), and preexponentials obtained from transition-state theory (TST) or available surface science experiments. Simulations are performed using this trial reaction mechanism with various reactor scale models, in order to predict different types of experimental data. Feature identification tools are used in order to identify the important reactions for each experiment. Finally, the rate constants of these important reactions are optimized, in order to minimize the distance between the experimental data and the corresponding model responses. The applicability of the optimized mechanism over a wide range of operating conditions is confirmed by validation against additional experimental data and uncertainty analysis. In addition, experiments and/or theoretical calculations needed to clarify important features can be proposed. These steps are now elaborated in the remainder of this section.

Construction of an initial mechanism

Based on analogy to existing detailed gas-phase reaction mechanisms and compilation of various data in the literature, a comprehensive set of reactions that can occur on the surface is first set up. All possible paths for the formation of a species are considered. This feature is essential in order that the mechanism be elementary-like and thus applicable over a wide range of conditions. Naturally, different pathways may become dominant under different conditions (Bui et al., 1997b). For example, prior to H_2 ignition, O_2 adsorption or H^* desorption is the rate-limiting step, but H_2 adsorption

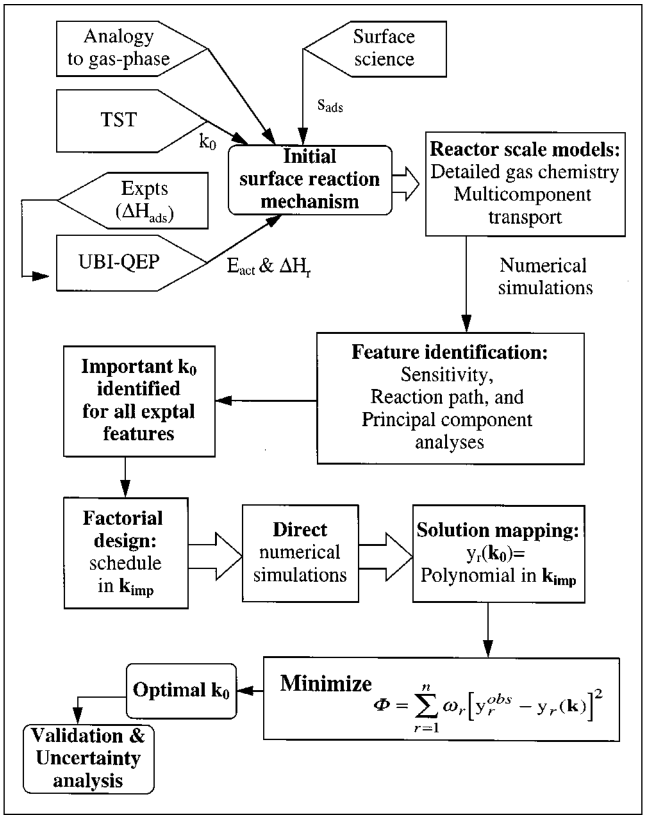

Figure 1. Methodology for detailed surface-reaction mechanism development.

The unity bond index–quadratic exponential potential method is used to compute thermodynamically consistent, species-coverage-dependent activation energies and heats of reactions for the entire mechanism. Mathematical analysis determines the important reactions for each experimental feature analyzed, and preexponentials of these important reactions are optimized for the best prediction of the experiments. Solution mapping and factorial design techniques are used to render the multiparameter, multi-data-set optimization problem computationally feasible. Finally, the optimized mechanism is validated against experimental data.

usually becomes rate-determining after ignition. In addition, due to the speed of the oxidation reactions and the high coverages encountered, the common assumption of the partial equilibrium of the adsorption–desorption steps is invalid under interesting, practical conditions. For this reason, no assumptions about a rate-limiting step are made, that is, the full reaction mechanism is numerically solved. Furthermore, derivation of an analytical, complex rate expression of the Langmuir-Hinshelwood type does not necessarily simplify either computational cost or programming, as the former is usually determined by fluid-phase chemistry, and the latter is straightforward and done only once for elementary reaction mechanisms (only the reaction mechanism input has to be changed). In a complex reaction network the rate-limiting step can easily be identified by the sensitivity analysis tools discussed below. In most cases, more than one step can significantly contribute to the rate of production of the desired product. In our mechanism, all surface-reaction steps are elementary, bi-, or unimolecular.

For the adsorption steps, surface science experiments from the literature are used to obtain the initial values of sticking coefficients (s_{ads}). Since these experiments are typically conducted at ultrahigh vacuum conditions, using well-characterized single-crystal surfaces, available sticking-coefficient values provide an estimate for practical operating conditions. The experiments of various groups, over different single-crystal and polycrystalline surfaces (in order to at least partially address the issue of materials gap), are compiled, wherever possible, to find the ranges of reasonable values for sticking coefficients. While the roles of support and multiple crystallographic planes for structure-sensitive reactions cannot be downplayed, in the absence of available data on real catalysts, data on the most common facets—(111) and (100), for example—could be good initial guesses for optimization.

For the remaining steps of the mechanism, transition-state theory is applied in order to obtain initial estimates for the preexponentials (assumed to be temperature and coverage-independent). Reliable data from surface science experiments can also be used whenever available. Even though preexponentials can vary with temperature and coverage, the corresponding change in the reaction rate constant due to the activation energy is typically much higher (Shustorovich and Sellers, 1998). In our analysis, for the desorption steps, both associative (such as $2H^* \rightarrow H_2 + 2^*$) and molecular (such as $H^* \rightarrow H + ^*$), a value of $10^{13}\ s^{-1}$ is used, whereas for the Langmuir – Hinshelwood-type bimolecular reactions (such as $C^* + H^*) \rightarrow OH^* + ^*$), a value of $10^{11} s^{-1}$ is used. These values correspond to an average of the transition-state theory estimates based on the general reactions of each type (Dumesic et al., 1993). As numerical simulations demonstrate below, these estimates are sufficient to construct a quantitative surface-reaction mechanism.

In the next step, the heats of chemisorption of all species involved in the surface-reaction mechanism are compiled from experiments from the literature as a function of species coverage. In order to ensure thermodynamic consistency within the mechanism, we calculate the heats of all reactions as linear combinations of heats of adsorption of species (number of linearly independent reaction heats) and the enthalpies of species in the corresponding gaseous reactions. In this way, the effect of adsorbate–adsorbate interactions on the heats of reactions is easily and correctly accounted for. To our knowledge, this is the first time this has been done. A large pool of thermodynamic data exists for hydrogen, oxygen, water, and other simple molecules on noble metals of interest to catalytic oxidation [see Park et al. (1999) for details on the H_2/O_2 reaction on Pt].

Based on the work of Shustorovich and coworkers (Shustorovich, 1990; Shustorovich and Sellers, 1998), using the heats of chemisorption as inputs, a thermodynamically consistent set of activation energies is derived for the proposed detailed surface reaction scheme using the UBI–QEP method. In addition, we have extended this formulation to situations involving coverage-dependent heats of adsorption, to derive coverage-dependent activation energies and reaction heats for the entire mechanism, while maintaining thermodynamic consistency. Further details are provided in (Park et al., 1999). The activation energies and reaction heats are computed on the fly within our codes, and are not subsequently adjusted. We should remark that this approach to mechanism construction can explain, at least in part, large differences in the reported activation energies of some reactions by their strong coverage dependence. Examples include the reactions $H_2O^* + O^* \rightarrow 2OH^*$ and $H_2O^* + ^* \rightarrow H^* + OH^*$, where the activation energy can change by ~ 20 kcal/mol, due to adsorbate−adsorbate interactions (Park et al., 1999).

In our methodology, the choice of the semiempirical UBI−QEP method for calculating the activation energies of the surface reactions is dictated by its computational speed and reasonable accuracy for a large number of reactions observed after testing against experiments by its developers. Examination of the UBI−QEP-derived activation energies shows that they agree well with experimental data for a number of reactions considered here (Park et al., 1999). While use of *ab initio* and, in particular, density functional theory (DFT) has many merits (Sautet and Paul, 1991; van Santen, 1991; van Santen and Neurock, 1997), its application to a large reaction network is beyond currently available computational capabilities, and the connection of low index plane energetics to polycrystalline or supported catalysts may not be trivial. As a result, we believe that validation of important paths identified here and use of DFT to calculate unavailable heats of chemisorption will be invaluable contributions to our methodology as more complex fuels are considered.

Experiments and reactor scale models

To develop a comprehensive reaction mechanism, different experimental data (multidata and multitypes of experiments) should be considered. We distinguish here between ‘‘engineering type’’ and ‘‘fundamental type’’ data. The former, such as ignitions, extinctions, selectivities, and conversions are of practical interest and should be quantitatively reproduced. The latter, such as low-pressure laser induced fluorescence (LIF) data of hydroxyl mole fraction and other spectroscopic data, are useful in optimizing and validating complex reaction mechanisms. Availability of such data as a function of important operating parameters (e.g., composition, pressure, flow rate) is essential for mechanism discrimination through important feature identification discussed in the next section. While not all of these data are needed, it is important that a minimum number are available for optimization.

An appropriate reactor scale model is needed to model each type of experiment. The initial surface-reaction mechanism developed is used as a satellite (subroutine) to appropriate reactor scale models that can include multicomponent species and energy transport, fluid mechanics, and gas-phase chemistry features. For example, the laminar, stagnation-point flow model (Bui et al., 1997a) is used for experiments conducted on catalyst foils. To describe molecular-beam experiments, a simple gradientless reactor model, with surface reactions only (no gas-phase reactions), is used. Several other configurations, such as a CSTR or a two-dimensional tubular reactor model, are used when appropriate. These reactor scale models are of different mathematical forms, including algebraic equations, initial, or boundary value problems. The outcome of the reactor scale model is the direct prediction of various experimental data of interest.

Mathematical analysis for feature identification

For each type of experiment modeled, mathematical tools such as sensitivity and reaction-path analyses are used in order to identify the important reactions governing the predictions. Sensitivity analysis involves perturbation of preexponentials from their nominal, initial value, and estimation of the corresponding change in the model response. Various types of sensitivity analysis and associated algorithms exist that are appropriate for regular or singular (bifurcations) solutions, local or global in nature, brute force or not, and the like [e.g., Yetter et al., 1991; Tomlin et al., 1997; Kalamatianos et al., 1998]. Aside from providing insight into the governing physics, sensitivity analysis determines the subset of important preexponentials, k_{imp}, that can be optimized based on a specific set of experimental data. Obviously, if all the desired model responses are insensitive to a certain rate constant, there is no physical justification for including it in the optimization. Sensitivity analysis also delineates apparently different experiments which, however, provide a similar set of important parameters (redundant information). In such cases, only one of these experiments can be used in optimization (targeted experiment), whereas the rest can be used to validate the mechanisms of different operating conditions, as discussed below.

Aside from experimental values, specific features of the data can also be chosen to determine the important steps. For example, the slope of the inlet fuel mole fraction vs. surface-temperature curve may be used. In the case where the experimental data show a change in the slope upon varying an operating parameter (such as inlet composition), the two limiting slopes, and/or the value of the operating parameter where the slope changes, are additional features that may be chosen for sensitivity analysis. Below we provide examples of such sensitivity analysis, as they pertain to the H_2/air reaction over Pt.

Solution-mapping and global optimization for mechanism refinement

In order to obtain an optimized set of preexponentials, the mathematical problem is formulated as finding the global minimum of the weighted least-squares objective function.

$$\phi = \sum_{r=1}^{n} \omega_r \left[y_r^{\mathrm{obs}} - y_r(k) \right]^2, \tag{1}$$

where n is the number of experimental observations, ω_r is the weight assigned to the rth measurement, y_r^{obs} and $y_r(k)$ are the rth experimental and model-predicted quantity, respectively, and k is the vector of reaction preexponentials. Here Φ is the total distance between the experiments and the corresponding model predictions. The weights have to be picked based on the reliability and importance of the corresponding experiment, and set to 1.0 for all observations where such information cannot be determined. The y_r^{obs} can typically include ignition temperatures, selectivities and conversions, LIF data on mole fraction of OH, or any other experimentally measurable quantity. Aside from reaction preexponentials, heats of chemisorption can also be used as optimization parameters. We prefer reaction preexponentials, as each reaction can be optimized independently (in principle, the heat of chemisorption affects many reactions, according to the UBI−QEP framework) and the activation energies account for most of the temperature effects in the experiments.

Aside from the issue of global optimality, optimization of the large-reaction networks is nontrivial for the following reasons: First, the model predictions $y_r(k)$ are obtained as the solution of a heterogeneous set of equations applicable to each experimental setup under consideration, and may include systems of algebraic equations, ordinary differential equations (ODEs), partial differential equations (PDEs), and differential-algebraic equations (DAEs). Different codes typically exist for each reactor configuration, making simultaneous optimization difficult. Second and most important, effective global optimization algorithms may involve a large number (on the order of 100,000) of function evaluations (Corana et al., 1987; Goffe et al., 1994). This can make the problem of minimizing Φ prohibitively computationally expensive, especially when a submodel involves two-dimensional detailed transport-chemistry-solver calls (very expensive function evaluations). Third, the reactor scale model codes are often not robust enough to be used as subroutines of a global optimization program.

To overcome these obstacles, we therefore propose, instead of a direct optimization, an indirect one, involving factorial design, solution-mapping, and linear regression, as detailed below. In the gas-phase kinetics analog of our problem, a method called ‘‘solution-mapping’’ has been found to be effective (Miller and Frenklach, 1983; Frenklach, 1984; Frenklach and Miller, 1985; Frenklach et al., 1992; Eiteneer et al., 1998) in the systematic optimization of multiparameter, multidata, multitype model responses. In this method, the solution of the model equations is decoupled from the optimization problem by deriving simple, empirical expressions for the responses y_r as functions of k_{imp}. This technique is sometimes also referred to as response surface methodology (Myers, 1981; Sacks et al., 1989a,b; Helton, 1993) and is directly linked to the preceding sensitivity analysis. Since the surface chemistry is typically used as a boundary condition in large-scale simulations, the use of solution mapping reduces the computational cost of our methodology determined primarily from the solution of PDEs, which is in turn affected by the number of species in gas-phase rather than surface chemistry. Thus application to large hydrocarbons should be feasible. Given an initial mechanism, large-scale simulations can be performed to obtain y_r. We use factorial design in order to determine an optimal schedule of sampling points for performing simulations involving changes in all the important k's. This technique is based on the work of Box and Draper, and was formulated as a means of determining an optimal set of experiments for parametric studies in cases where the measured quantity is strongly dependent on more than one operating condition (Box and Draper, 1987). For a problem in m dimensions, that is, involving m operating parameters (k's in our case), factorial design indicates that there are 2^m sample points. Using this design schedule, reactor-scale simulations are performed, and a table of y_r vs. k_{imp} is obtained. Regression analysis is then used in order to develop polynomial fits for y_r, with a minimum number of computations. At the same time, as long as the polynomial fits are good, the essential features of the detailed model are not lost.

In our study, we have used scaled variables in place of the original preexponentials

$$x = \ln\left(\frac{k^2}{k_{\min}k_{\max}}\right) \Big/ \ln\left(\frac{k_{\max}}{k_{\min}}\right), \tag{2}$$

where a preexponential k in the interval $[k_{\min}, k_{\max}]$ is mapped to x in the interval $[-1,1]$. This scaling is convenient, as it converts all the parameters that can differ by many orders of magnitude (e.g., sticking coefficients and reaction preexponentials) to the same range of values. The sticking coefficients are changed within the limits of existing experimental values, whereas the preexponentials are typically changed by up to two orders of magnitude, with the initial transition-state theory estimate (or an available experimental value) at the center of the interval. Using such large perturbations, we compromise between local sensitivity analysis, which entails infinitesimal perturbations, and global sensitivity analysis, which spans the entire parameter space with simultaneous perturbations in all parameters. Even though the latter sensitivity analysis is superior, it is computationally very demanding. Preexponentials of surface reactions may significantly differ from these values, an issue addressed in the methodology in the final, self-consistency test. We should mention that choosing a large window of variation of the k's is beneficial, in that the optimal k value is more likely to be enclosed, although at the expense of the accuracy of the fits.

A typical design schedule for three variables is indicated in the left part of Table 1. Apart from the 8 points determined by factorial design, additional ones have been incorporated in order to improve the polynomial fits. The ODRPACK package has been used to obtain second-order polynomials in the scaled variables, for all the experimental data analyzed (Boggs et al., 1989). The polynomial fits are always $< 0.01\%$ of the large-scale simulation responses regarding ignition and $< 3\%$ at some of the vertices of the training box for the LIF data. Finally, simulated annealing is used for the multiparameter, multi-data-set global optimization of the preexponentials (Corana et al., 1987; Goffe et al., 1994). By performing the optimization with different initial guesses, convergence to

Table 1. Factorial Design Table for Ignition Temperature of H_2/Air Mixtures Over Polycrystalline Pt*

Sample	$H_2/(H_2+O_2)$			0.2	0.3	0.4	0.5
No.	X_1	X_2	X_3	T_1 (K)	T_2 (K)	T_3 (K)	T_4 (K)
1	−1.0	−1.0	−1.0	390	412	431	—
2	1.0	−1.0	−1.0	417	441	465	495
3	−1.0	1.0	−1.0	304	341	359	373
4	1.0	1.0	−1.0	354	372	386	400
5	−1.0	−1.0	1.0	314	324	333	342
6	1.0	−1.0	1.0	325	337	348	358
7	−1.0	1.0	1.0	269	286	294	341
8	1.0	1.0	1.0	290	298	306	313
9	2.3	−1.0	−1.0	358	378	394	412
10	2.3	−1.0	1.0	297	306	314	321
11	0.0	0.0	0.0	333	347	359	370
12	0.0	1.0	0.0	308	323	334	344

**Note:* X_1, X_2, and X_3 are the transformed variables corresponding to the sticking coefficient of H_2, the sticking coefficient of O_2, and the H* desorption preexponential, respectively. The sampled ignition temperatures at four inlet fuel compositions are also shown.

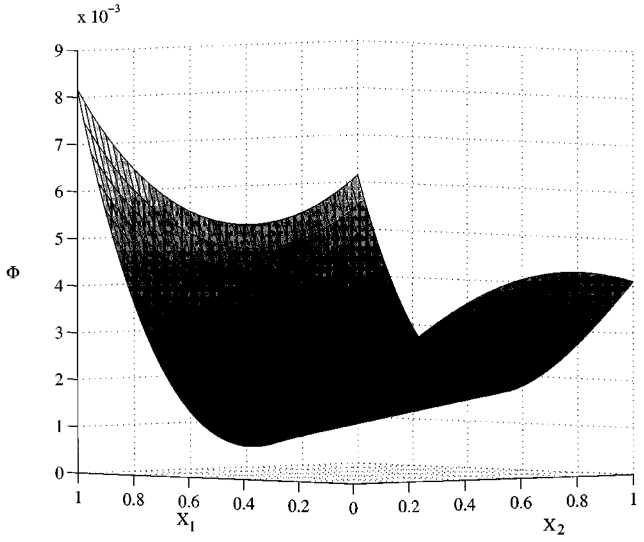

Figure 2. Objective function Φ for the ignition temperature data as a function of the scaled variables corresponding to sticking coefficients of H_2 (axis X_1) and O_2 (axis X_2).

The value of the H* desorption preexponential has been kept fixed at 9.4 10^{11} s^{-1}, for this plot. A "fold"-like minimum is observed, indicating that the optimal solution is nonunique using only these types of data.

the same minimum was verified. Typically, for a problem involving eight optimization variables, 500,000 function evaluations are involved in an optimization that take about 10 min on a 500-MHz DEC machine. The annealing schedule has to be strict enough to prevent convergence to local minima (Goffe et al., 1994). A quenching rate of 0.999 was used in the calculations here. The results of the simulated annealing were compared to ODRPACK routines (Boggs et al., 1989), primarily for statistical analysis (see below).

The shape of the objective function in the parameter space gives an indication of the uniqueness of the optimum. Since it is not practical to do this for more than two parameters, we have examined surfaces, keeping all but two of the parameters fixed at their optimal values. In some cases, features of the nonuniqueness of the optimum have been identified. For example, at a specific preexponential value for H* desorption, the objective function surface for ignition temperatures plotted as a function of the sticking coefficients of H_2 and O_2 is seen to possess a long foldlike minimum, along which the ratio of the sticking coefficients is found to be a constant (see Figure 2). It turns out that this is consistent with an analytical ignition criterion for H_2/O_2 (Bui et al., 1977b) (and similar ones for paraffins; Aghalayam and Vlachos, 1999; Trevino, 1999), that show that the ratio of sticking coefficients, rather than the individual sticking coefficients, is the controlling parameter. Both sticking coefficients can be determined by using additional experimental data (for which only one of the two parameters is important).

Validation and self-consistency of the optimized mechanism

Once an optimized set of preexponentials is obtained, large-scale simulations are conducted with this new surface-reaction mechanism to obtain model predictions for different experimental data. In particular, sets of data that have not been included in the optimization because they were redundant, but are nevertheless important, have to be considered in order to ensure that the mechanism is widely applicable. Also, as a self-consistency check, sensitivity analysis can be performed with the optimized mechanism and the results compared with those of the original sensitivity analysis. In general, sensitivities of various features to the preexponentials have to be obtained to ensure that important steps were not left out in the solution mapping. Furthermore, the optimal values of preexponentials should be within the box used in the factorial design so as to accurately represent the model responses in the optimization step. Otherwise, an iterative scheme can be employed, where the initial training box is suitably adjusted, and the preceding procedure is repeated. Finally, identification of important controversial paths that may not have been previously studied provides feedback for further experimental studies or DFT calculations, as mentioned earlier. We have recently demonstrated this latter issue for methane oxidation on Pt (Aghalayam et al., 2000). Other important aspects that are analyzed once an optimized mechanism is obtained are the statistical significance of the results and the influence of various uncertainties in the methodology, on the final estimated parameters.

New Detailed Reaction Mechanism for Hydrogen/Air Mixtures on Polycrystalline Pt

Contruction of the initial reaction mechanism

In order to validate our approach, we have considered the H_2/air reaction on Pt. This system has been fairly thoroughly studied, and while many mechanisms have been published, they are either thermodynamically inconsistent or cannot accurately predict multiple experimental data. However, the reaction steps are well-established. Figure 3 shows the mechanism, which consists of a total of 18 steps. It involves the dissociative adsorption of H_2 and O_2 onto the Pt surface. The surface species H* and O* can either react on the surface to form OH*, or desorb to give the corresponding stable

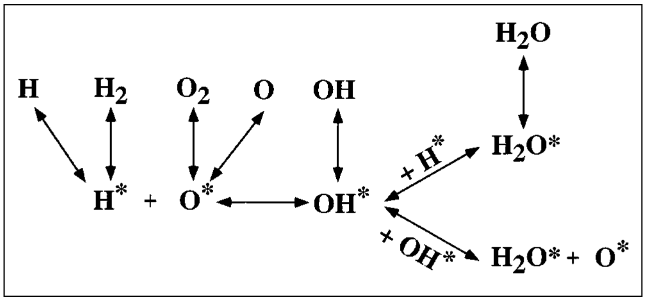

Figure 3. Detailed surface-reaction mechanism for the oxidation of H_2 over Pt catalyst.

* Denotes an adsorbed species. H_2 and O_2 dissociatively adsorb on the surface to form H* and O*, respectively. These species react on the surface to produce OH*, which can in turn form water through two different pathways. The radical species H and O in the gas can also adsorb to give H* and O*, respectively. Finally, all surface species can desorb to give corresponding gas-phase species.

molecules (H_2, O_2) or radicals (H, O) in the gas phase. The OH^*, in turn, can desorb, or, depending on the conditions, form H_2O* through two possible paths. The water can then desorb into the gas phase. Table 2 shows all the reactions involved, along with the initial and optimized preexponentials. We should mention that using the UBI–QEP framework, the activation energies for all reactions in the mechanism change often as nonlinear functions of coverage (in contrast to the traditional linear functionality employed in desorption steps in the literature). Typical values for the vacant-site dominated case are indicated in Table 2.

Three types of adsorbate–adsorbate interactions are considered, based on available experimental data, namely, H^*-H^*, O^*-O^*, and OH^*-O^*, as in our earlier article (Park et al., 1999). The adsorption steps in this mechanism are considered to be nonactivated, and the coverage-dependent activation energies (in kcal/mol) for the desorption steps have been set based on experimental data:

$$E_d(H^*) = 20.0 - 6.0\theta_{H^*} \tag{3}$$

$$E_d(O^*) = 51.0 - 32.0\theta_{O^*} \tag{4}$$

$$E_d(OH^*) = 63.0 - 33.0\theta_{O^*} \tag{5}$$

$$E_d(H_2O^*) = 10.0, \tag{6}$$

where θ denotes the surface coverage of the species.

The sticking coefficients for the adsorption of H_2 and O_2 are expected to be in the 0.25–1.0 and 0.01–0.1 range, respectively (Park et al., 1999). We have chosen initial values of 1.0 and 0.1, respectively. For OH and H_2O, sticking coefficient values of 1.0 and 0.7, respectively, have been used (Park et al., 1999). The preexponentials of all surface reactions are then fixed at their initial values, as indicated in the previous section, and varied by two orders of magnitude (the minimum and maximum values chosen are an order of magnitude lower and higher, respectively, than the nominal value).

Table 2. Catalytic H_2 Oxidation Mechanism on Platinum[**]

	Reaction	Preexponential (s^{-1}) or Sticking Coeff.			E_{act} (kcal/mol) $\theta^* = 1.0$
		Initial	Optimized		
(1)	$OH^* + ^* \rightarrow H^* + O^*$	1.0×10^{11}	6.1	$\times10^{11}$	24.4
			6.1 ± 1.4[††]	$\times10^{11}$	
			[4.5; 8.1][‡]	$\times10^{11}$	
(2)	$H^* + O^* \rightarrow OH^* + ^*$	1.0×10^{11}	1.7	$\times10^{10}$	12.1
			1.7 ± 0.5[††]	$\times10^{10}$	
			[1.3; 2.2][‡]	$\times10^{10}$	
(3)	$H_2O^* + ^* \rightarrow H^* + OH^*$	1.0×10^{11}	1.2	$\times10^{10}$	18.4
			1.2 ± 0.2[††]	$\times10^{10}$	
			[1.1; 1.5][‡]	$\times10^{10}$	
(4)	$H^* + OH^* \rightarrow H_2O^* + ^*$	1.0×10^{11}	3.5	$\times10^{11}$	12.4
			3.5 ± 0.8[††]	$\times10^{11}$	
			[2.8; 4.6][‡]	$\times10^{11}$	
(5)	$H_2O^* + O^* \rightarrow 2OH^*$	1.0×10^{11}	1.0	$\times10^{11}$	12.6
(6)	$2OH^* \rightarrow H_2O^* + O^*$	1.0×10^{11}	1.0	$\times10^{11}$	18.9
(7)	$H_2 + 2^* \rightarrow 2H^*$	1.00	0.48		0.0
			0.48 ± 0.3[††]		
			[0.44; 0.52][‡]		
			0.52[‡‡]		
(8)	$2H^* \rightarrow H_2 + 2^*$	1.0×10^{13}[†]	9.4	$\times10^{11}$	20.0
			9.4 ± 5.0[††]	$\times10^{11}$	
			[7.9; 11.0][‡]	$\times10^{11}$	
			2.5[‡‡]	$\times10^{11}$	
(9)	$O_2 + 2^* \rightarrow 2O^*$	0.10	0.03		0.0
			0.03 ± 0.005[††]		
			[0.027; 0.035][‡]		
			0.02[‡‡]		
(10)	$2O^* \rightarrow O_2 + 2^*$	1.0×10^{13}	1.0	$\times10^{13}$	51.0
(11)	$H_2O + ^* \rightarrow H_2O^*$	0.70	0.70		0.0
(12)	$H_2O^* \rightarrow H_2O + ^*$	1.0×10^{13}	1.0	$\times10^{13}$	10.0
(13)	$OH + ^* \rightarrow OH^*$	1.00	1.00		0.0
(14)	$OH^* \rightarrow OH + ^*$	1.0×10^{13}	1.0	$\times10^{13}$[*]	63.0
(15)	$H + ^* \rightarrow H^*$	1.00	1.00		0.0
(16)	$H^* \rightarrow H + ^*$	1.0×10^{13}	1.0	$\times10^{13}$	60.2
(17)	$O + ^* \rightarrow O^*$	1.00	1.00		0.0
(18)	$O^* \rightarrow O + ^*$	1.0×10^{13}	1.0	$\times10^{13}$	67.0

[*] Removed from optimization set and reset to initial value.

[**] The initial estimate and the final optimized values of the preexponentials and sticking coefficients for each reaction are indicated, along with the activation energy for a vacancy-dominated surface.

[†] Since the optimized value obtained was outside the original range chosen, this value has been reduced by an order of magnitude in the initial mechanism.

[††] Effect of uncertainty in experimental data.

[‡] Ninety-five percent confidence intervals of optimized preexponentials.

[‡‡] Uncertainty due to a 10% variation in heat of chemisorption of H_2.

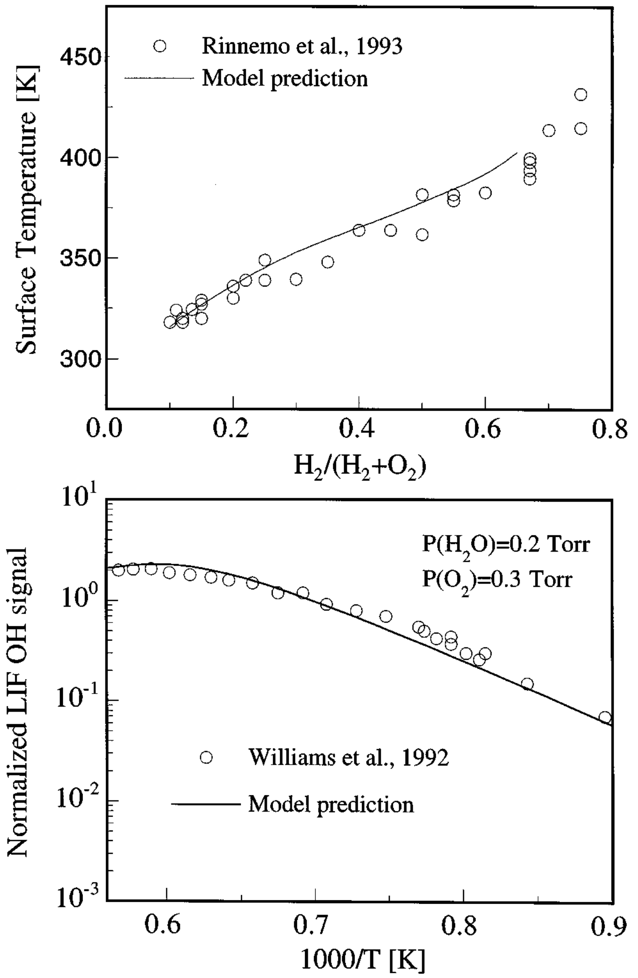

Figure 4. Experimental data vs. model predictions using the optimized reaction mechanism.

(a) For ignition temperatures as a function of the inlet fuel composition (conditions of atmospheric pressure, 5 s^{-1} strain rate, and 94% N_2 dilution); (b) for low-pressure LIF data of OH mole fraction as a function of the surface temperature (reactor pressure of 0.2 torr of H_2O and 0.3 torr of O_2). The model predictions are in good agreement with the experimental data.

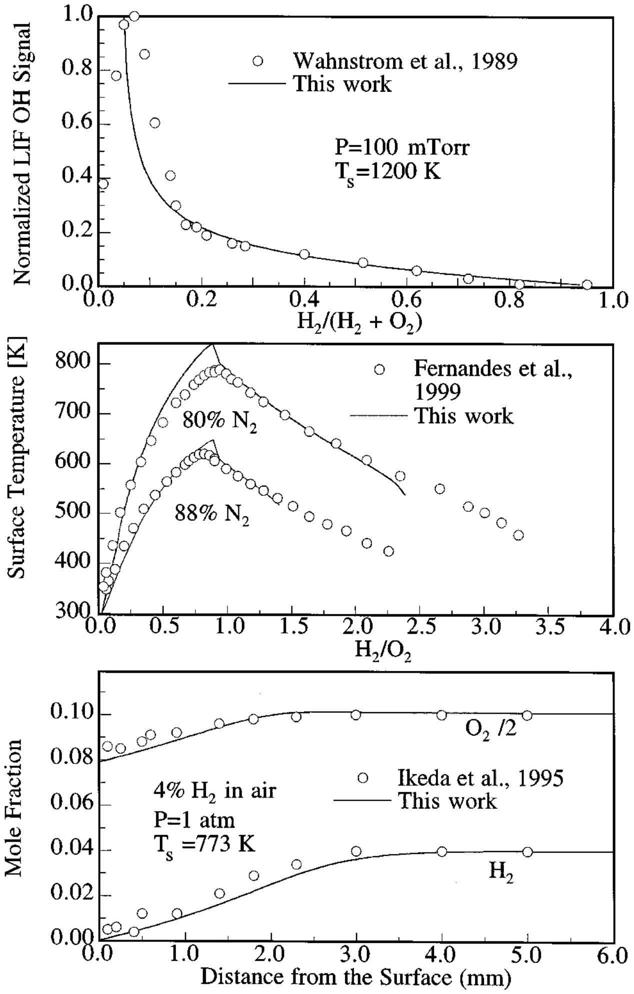

Figure 5. Model predictions vs. experimental data.

(a) OH mole fraction as a function of the inlet fuel composition, at a total reactant pressure of 200 mtorr and a surface temperature of 1,200 K; (b) autothermal temperatures as a function of the inlet fuel composition, for a Pt foil, at a strain rate of 5 s^{-1}, and different levels of N_2 dilution; (c) species mole fraction profiles along the length of the reactor, at atmospheric pressure, 31 s^{-1} strain rate, a surface temperature of 773 K, and 4% H_2/air mixture at the inlet: for all cases, the model predictions are in good agreement with experimental data, validating the optimized mechanism.

Experimental data

The available experimental data for H_2 oxidation on polycrystalline Pt consist of ignition temperatures as a function of fuel composition (Rinnemo et al., 1993; Deutschmann et al., 1995), OH mole fraction as a function of catalyst temperature (Williams et al., 1992) and inlet fuel composition (Wahnström et al., 1989) at low operating pressures, autothermal temperatures at various N_2 dilution levels (Fernandes et al., 1999), and spatial concentration profiles of the reactants (Ikeda et al., 1995), also summarized in our earlier publication (Park et al., 1999). Figures 4 and 5 show these data in symbols.

The experimental ignition data in Figure 4a indicate that H_2 inhibits ignition, that is, ignition temperatures increase with increasing inlet H_2 composition. These experimental data are representative of ignition temperatures of H_2 on Pt. In particular, comparison with data of other groups shows reasonable agreement between experiments. However, scatter of ±50 K is also noticeable in the ignition temperatures and terminal points of hysteresis, and is probably caused by the structure-sensitive nature of this reaction on Pt (see also Fernandes et al., 1999). Figure 4b shows the LIF OH mole fraction as a function of surface temperature. Two distinct regimes can be seen: at low temperatures, the OH mole fraction is strongly temperature-dependent, while at higher temperatures, the curve is relatively flat, showing little variation in temperature.

Figure 5a shows that the OH mole fraction goes through its maximum as the inlet fuel composition is increased, and that the OH mole fraction is low over most of the fuel-rich regime. Figure 5b shows the autothermal temperatures at two different N_2 dilutions, with a maximum at the surface stoi-

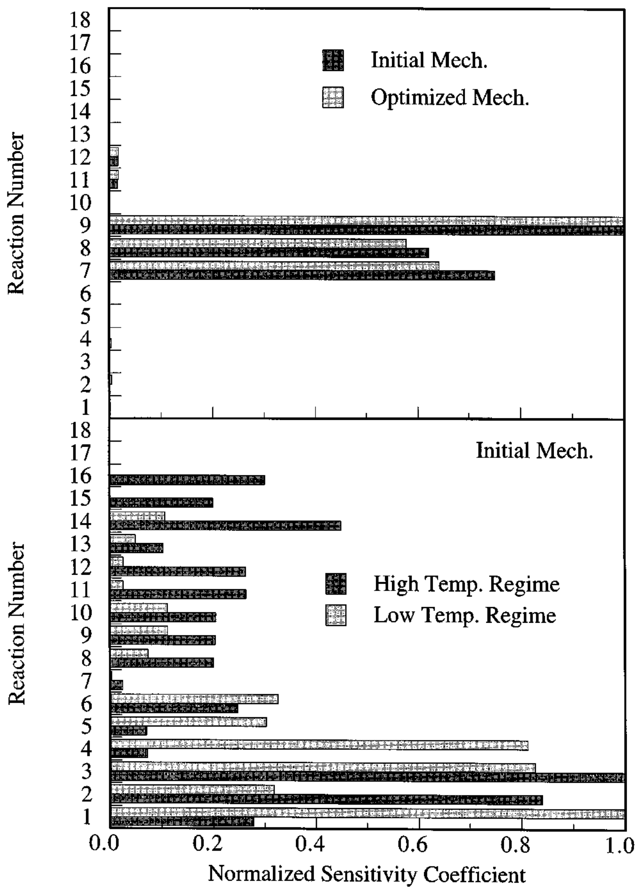

Figure 6. Sensitivity analysis of: (a) important steps for ignition temperature, at an inlet H_2 composition of 3%, and N_2 dilution of 94%, using both the initial and final optimized mechanisms; (b) LIF OH mole fraction as a function of the surface temperature at high and low temperatures.

The reaction numbers correspond to the ones in Table 2. In both cases, the adsorption of H_2 and O_2, and the desorption of H* are crucial, whereas all the other steps in the mechanism are of minor importance.

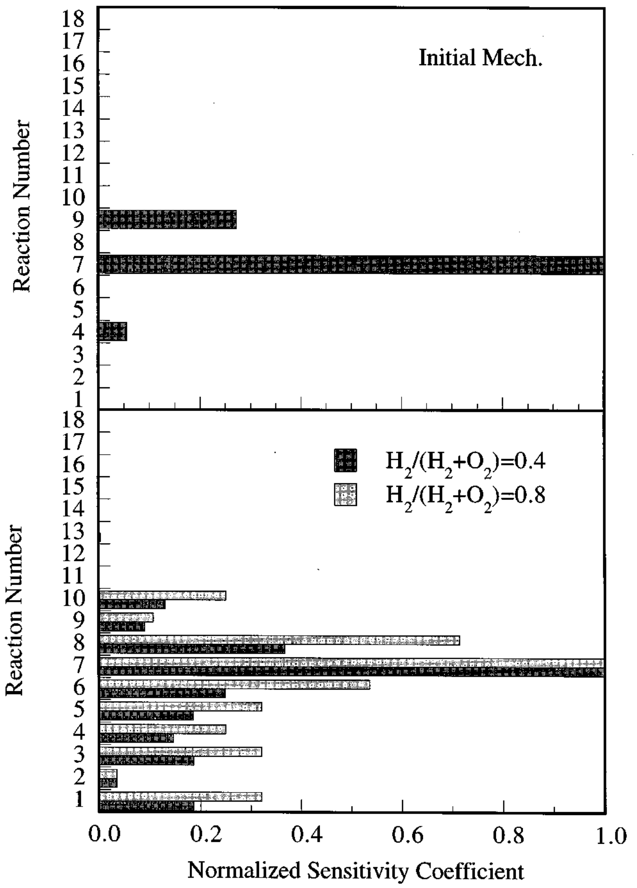

Figure 7. Sensitivity analysis of LIF OH mole fraction vs. inlet fuel composition.

The reaction numbers correspond to those in Table 2. (a) The position of the maximum is only sensitive to the adsorption of hydrogen and oxygen, whereas (b) the OH mole fraction at high inlet H_2 compositions is sensitive to a number of steps.

chiometric point. Finally, Figure 5c shows the profiles of H_2 and O_2 measured as a function of the distance from the catalyst surface.

We choose only some of the available data for the purpose of the optimization (targeted experiments) and leave the rest (redundant) for subsequent validation of the optimized mechanism. This choice is based on a screening sensitivity analysis, which is discussed next.

Screening sensitivity analysis

Figure 6a shows the normalized sensitivity analysis for the ignition temperature at an inlet composition of $H_2/(H_2+O_2) = 0.5$. Figure 6b shows the sensitivity analysis for the slope of LIF OH vs. temperature data (shown in Figure 4b) in the high and low temperature regimes. Finally, Figure 7 shows the sensitivity of the position of the maximum (panel a) and the values at two points (panel b) in the tail of the LIF OH mole fraction vs. composition data (shown in Figure 5a). The absolute value of the brute-force sensitivity coefficient is defined as

$$\left| \frac{Y(k_{\text{perturbed}}) - Y(k_{nominal})}{Y(k_{nominal}).} \right| \qquad (7)$$

The sensitivity coefficients are all normalized with respect to the largest one for each data set, so that the maximum value in each case is 1.0. For the results shown in Figures 6 and 7, the kinetic parameters have been perturbed from their nominal value by an order of magnitude.

The ignition temperature is sensitive to the adsorption steps of H_2 and O_2 and the desorption of H*. The OH vs. temperature data are sensitive to the OH* desorption step and formation—destruction steps of OH* and H_2O on the surface. Overall, LIF data provide a wealth of information about the kinetic mechanism compared to ignition data. The position of the maximum in the OH vs. composition data is also sensitive to the sticking coefficients of H_2 and O_2, whereas the tail is sensitive to H_2 adsorption−desorption and H_2O^* formation−destruction from OH^*. The composition LIF data provide nearly redundant kinetic information compared to the ignition and temperature LIF data, and can be used for validation. This choice is based on the fact that a larger number of experimental ignition data points are available, and that from a practical point of view, ignition is important to predict (for start-up and safety of the reactor). Aside from adsorption−desorption parameters, the autothermal temperatures are mainly transport-controlled (Fernandes et al., 1999), as are the species spatial profiles, and so we do not consider these data for the optimization of the kinetics.

The LIF OH vs. surface temperature and the ignition temperatures together are chosen as optimization targets. Additional experiments are needed to refine the parameters of the rest of the steps listed in Table 2. For example, detection of H, O, H^*, O^* can provide information about radical coupling with the gas phase. The choice of a specific species can be guided by sensitivity analysis of the species concentration using our optimized mechanism.

Solution mapping: Factorial design and polynomial fits

For ignition, the corresponding factorial design schedule in the sticking coefficients of H_2 and O_2 and the H^* desorption preexponential, along with some of the sampled ignition temperatures (at inlet compositions of $H_2/(H_2+O_2) = 0.2$, 0.3, 0.4, and 0.5), are indicated in Table 1. Polynomial fits are obtained for the ignition temperature at each composition ratio. As an example, the polynomial fit at $H_2/(H_2+O_2) = 0.5$ is

$$T_{\text{ign}}(K) = 370 + 10.75X_1 - 3.56X_2 - 21.81X_3 - 11.05X_1^2 - 11.00X_1X_2 - 13.75X_1X_3 - 22.44X_2^2 - 7.94X_2X_3 - 23.80X_3^2. \quad (8)$$

For the LIF data, in the low temperature regime, k_1, k_3, and k_4 were chosen as the important parameters, while for the high temperature LIF data, k_2, k_3, and k_{14} were selected (as indicated in Figure 6b). Thus, as a first step, we have chosen the three preexponentials that give maximum sensitivity. Recognizing that, in the final analysis, others, such as k_{16}, k_6, and k_{11}, k_{12}, may have contributions for the high-temperature LIF data, we have included k_6 in the set of important k's for this regime, but finally left it out, as the optimized values were not significantly different from the initial one. The water adsorption−desorption parameters (k_{11} and k_{12}) are well-characterized experimentally (Thiel and Madey, 1987), hence we have left them out of the optimization, as they are anyway of secondary importance as compared to the other preexponentials. This is also in line with the recommendation of Frenklach et al., who suggested that the selection of the important parameters (also termed as active parameters) must be based on the certain knowledge of the parameter values (Frenklach et al., 1992). Furthermore, optimizing a large number of preexponentials also raises the issue of degrees of freedom, since the number of experimental observations considered has to be greater than the number of optimized parameters to ensure uniqueness of the optimum. Given this choice of important parameters, factorial design schedules similar to that for ignition were constructed for the LIF data at four different surface-temperature values, in each of the two temperature regimes. Overall, eight parameters have been refined.

Optimization of the mechanism

The joint objective function, with equal weights for all the chosen points, is then minimized to obtain the optimal k. The function used is

$$\phi = \left(\frac{T_{\text{ign}}^1}{333} - 1\right)^2 + \left(\frac{T_{\text{ign}}^2}{347} - 1\right)^2 + \left(\frac{T_{\text{ign}}^3}{360} - 1\right)^2 + \left(\frac{T_{\text{ign}}^4}{369} - 1\right)^2 + \left(\frac{Y_{\text{high}}^1 T}{2.07} - 1\right)^2 + \left(\frac{Y_{\text{high}}^2 T}{1.91} - 1\right)^2 + \left(\frac{Y_{\text{high}T}^3}{1.80} - 1\right)^2 + \left(\frac{Y_{\text{high}T}^4}{1.70} - 1\right)^2 + \left(\frac{Y_{\text{low}T}^1}{0.55} - 1\right)^2 + \left(\frac{Y_{\text{low}T}^2}{0.42} - 1\right)^2 + \left(\frac{Y_{\text{low}T}^3}{0.30} - 1\right)^2 + \left(\frac{Y_{\text{low}T}^4}{0.15} - 1\right)^2, \quad (9)$$

where T_{ign}^i are the polynomial fits to the ignition temperatures, Y_{highT}^i are the corresponding fits for the OH mole fraction at four surface temperatures in the high-temperature regime, and Y_{lowT}^i are the polynomial fits for the OH mole fraction at four surface temperatures in the low temperature regime.

Table 2 includes the optimized preexponentials. Figure 4 shows the model predictions obtained using this new mechanism. Very good agreement can be seen between the predictions and the experiments. Even though there is no guarantee that the proposed mechanism is globally optimum, it is consistent with multiset experiments, and the kinetic parameters are reasonable. The parameters determined are in reasonable agreement with the ones obtained by trial-and-error (Park et al., 1999). Below, this mechanism is further checked using various statistical means, and is finally used for predictions, without further adjustments.

Uncertainties in estimated kinetic parameters

In this section we discuss the possible sources of approximation/errors in estimating kinetic parameters. In general, uncertainties can be caused by many factors, such as the approximation of the reactor using a specific model, uncertainties in the transport coefficients (e.g., diffusivities), catalyst aging, different catalyst treatment, and aspects related to the proposed methodology. It is this latter case that is discussed below. Even though the reaction steps for the H_2/O_2 reaction are well known, we envision that uncertainty analysis and the ease of the BOC formalism can enable evaluation and elimination of alternative reaction paths.

Uncertainty in Experimental Data. In the absence of detailed error information about the experiments, the experimental error was assumed to be normally distributed with a standard deviation of $\sigma \sim 20$ K for ignition temperatures (thermocouple temperature uncertainties can be as high as 50 K; for normal distribution, this means that $3\sigma = 50$ K) and $\sigma \sim 0.1$ (arbitrary units) for the LIF vs. temperature data. Next, the optimization is redone for the extreme situation where *all* experimental data are at their lower and upper bounds. Uncertainty intervals have been determined based on the maximum deviation from the nominal optimized values of preexponentials/sticking coefficients. In all cases, these intervals are smaller than those chosen for the solution mapping, so there is no need to repeat it. Table 2 shows the results. Some of the estimated kinetic parameters are seen to be less certain than others. Overall, the assumed errors in experimental data cause an uncertainty up to a factor of 1.6.

Approximation in Replacing the Large-Scale Simulation Results with Polynomials. To assure quality of the optimization, the derived polynomials should reasonably represent the full model. We have examined a sample situation for this case, focusing on ignition temperatures alone. In particular, two sets of polynomials were developed, one with $< 0.01\%$ deviation from the large-scale simulations, and the other one with $\sim 5\%$ deviation. The optimized values obtained in this case are found to be quite similar to the original ones. Nevertheless, we believe that having good polynomial fits is essential. Furthermore, in our experience, the estimated coefficients from the ODRPACK codes (Boggs et al., 1989) must be successfully converged to have meaningful results. Recent research on the development of a response surface methodology (Jones et al., 1998) shows promise for constructing and validating response surfaces.

Uncertainty in Deducing the Optimum of the Least-Squares Objective Function. Statistical analysis of the optimized values has been performed in order to determine their level of certainty. Ninety-five percent confidence intervals are determined for each of the optimized parameters, using a standard Students *t*-distribution estimate [ODRPACK (Boggs et al., 1989) does this automatically]. Initial results indicated very large ranges of values for k_{14}. In other words, we cannot place much confidence in the determined optimal value of k_{14}. Therefore, we have subsequently eliminated k_{14} from the set of optimized parameters, and redone the optimization. The 95% confidence intervals for all optimized parameters are indicated in Table 1.

It is clear that all the parameters are well within acceptable certainty. One way to reduce the uncertainty in k_{14} and actually include it in the optimization is to find additional model-sensitive experiments to optimize against. Improvements in the solution mapping to obtain better polynomial fits and inclusion of more experimental points in the objective function, are other general means by which the confidence intervals can be shrunk. Since our mechanism performs reasonably well overall, we have not included these exercises. We have not attempted to construct joint-confidence regions for the optimized parameters, since the equations for joint-confidence regions for least-squares minimization are only approximate for second-order polynomial models [see Box et al. (1978)].

Uncertainty in Model Input Parameters (Heat of Chemisorption and Adsorbate−Adsorbate Interaction Energies). Here the values used for the heats of chemisorption and adsorbate−adsorbate interactions of various species have been obtained from various experiments in the literature. Some scatter in these parameters is generally seen between various reports in the literature, even for the same crystallographic plane. In the absence of information, further uncertainties are expected when the heats of chemisorption of polycrystalline surfaces are approximated with the values from the low index planes. Finally, while the activation energy computed by the BOC formalism from the intersection of Morse potential surfaces is typically within a few kcal/mol of experiments, one should keep in mind that it is semiempirical.

We have examined ignition temperatures as an example of providing a flavor of such effects. In particular, the heat of the chemisorption of hydrogen (in vacancy-dominated situations) has been changed, from the nominal 20 kcal/mol case to 18 kcal/mol. This choice was based on the fact that the heat of chemisorption of hydrogen is the most influential of all the species in predicting ignition temperatures. The values found for the three optimized kinetic parameters are indicated in Table 2. The results vary by as much as 1.5 times the original value, for a 10% variation in the input heat of chemisorption. Thus, it appears that among the sources of uncertainty in estimating preexponentials in our methodology, the assignment of heats of chemisorption is the most critical. This is not surprising, as the energetics of surface reactions, which are determined from the heats of chemisorption, account for the wide variation in reaction rates with temperature. Variation in these input parameters results in a different optimum set of preexponentials.

Validation and self-consistency of the optimized mechanism

Figure 5a shows the model predictions using the optimized mechanism (lines) for LIF OH signal as a function of the inlet composition. Excellent agreement between the experiments and the model predictions is seen for the tail of the data. However, some discrepancies are noticeable at lower compositions. The maximum position is determined by the ratio of the sticking coefficients of hydrogen and oxygen. While good prediction of the maximum position can be obtained by changing this ratio, doing so in turn affects the prediction of ignition temperatures (an underprediction of ignition temperatures by $\sim 2\%$ has been found). This situation indicates a possible difference in sticking coefficients due to differences in operating conditions between the two experiments or experimental uncertainty in the maximum of Figure 5a (and/or ignition data). Predictions of the autothermal temperatures as a function of the inlet fuel composition are plotted in Figure 5b. The differences seen in predicting the fuel-rich flammability limit are mainly attributed to the faceting occurring during the experiment that causes a change in the adsorption−desorption parameters of H_2. Finally, Figure 5c shows the species profiles at a fixed inlet composition and surface temperature. Our model predictions with the optimized mechanism are in good agreement with the experimental results.

Also, Figure 6a uses the optimized mechanism to show the sensitivity of the ignition temperature. The lack of significant differences between the original sensitivities and the final ones indicates that our initial mechanism was capable of qualitatively capturing the essentials of the experiment, and that the final optimized mechanism has not changed in this regard. Similar but greater differences in sensitivities have been found for the LIF data.

Conclusions

A new methodology has been proposed for mathematically rigorous optimization of a detailed surface-reaction mechanism capable of capturing the essentials of different experimental data over a wide range of operating conditions. Thermodynamic data from surface science experiments are used as inputs to the semiempirical, microkinetic UBI−QEP approach in order to obtain thermodynamically consistent, coverage-dependent activation energies and heats of surface reactions. Transition state theory estimates or experimental data are used as initial guesses for preexponentials. Screening sensitivity analysis of important features is then employed to determine the important parameters for each experimental set, by combining the initial surface reaction mechanism with the appropriate reactor scale models. Factorial design is subsequently used to determine an optimal schedule in the important preexponentials. Large-scale simulations are conducted based on this schedule, to obtain a table of model responses vs. important parameters, that is fitted using a low-degree polynomial. Global optimization is carried out in order to minimize the distance between experimental quantities and the polynomial fits, leading to an optimal set of preexponentials. Analysis of associated uncertainties is performed to ensure the quality of the optimized mechanism. We believe that these elements of solution mapping, optimization, and uncertainty analysis, introduced in this article for surface reactions, are essential for the construction of mechanisms for more complex fuels.

This methodology has been applied successfully to the H_2/air reaction over Pt, using a multiset of experimental data. We believe that the good performance of our mechanism over a wide range of operating conditions illustrates both the potential of our methodology for complex surface-reaction mechanism development, and the overall quality of the mechaism. While the underlying reaction steps (in terms of elementary reaction paths) in our mechanism are no different that the ones in the literature, the thermodynamically consistent, coverage-dependent activation energies and mathematically optimized preexponentials provide a superior mechanism, consistent with multiple experimental data. Given the experimental uncertainty and the fact that experiments from various groups with different catalyst pretreatments were simultaneously used or validated, the approach shows good promise. Even though not demonstrated here, the methodology allows for systematic screening of hypothetical reaction paths that are quantitatively consistent with the experimental data, while providing feedback for further experiments or theoretical validation. We have found such examples in the case of methane (Aghalayam et al., 2000), for which elementary steps are not well established, as will be discussed in a forthcoming publication. We believe that the methodology presented here would allow construction and optimization of surface-reaction mechanisms of more complex, technologically interesting fuels.

Acknowledgments

Acknowledgment is made to the Office of Naval Research with Dr. G. D. Roy through a Young Investigator Award under Contract N00014-96-1-0786, to the National Science Foundation (CAREER CTS-9702615 and CTS-9904242), and to NETI for financial support. We also wish to thank Prof. John Tsimikas of the University of Massachusetts Amherst for useful discussions on statistical analysis and Prof. Christodoulos Floudas of Princeton University for bringing to our attention the article of Jones et al. after submission of this manuscript.

Literature Cited

Aghalayam, P., Y. K. Park, and D. G. Vlachos, "Detailed Surface Reaction Mechanisms for Methane Oxidation on Platinum," *Proc. Joint Combustion Meeting of U.S. Sections of Combust. Inst.,* The Combustion Institute Washington, DC, p. 745 (Mar. 14−17, 1999).

Aghalayam, P., Y. K. Park, and D. G. Vlachos, "Partial Oxidation of Light Alkanes in Short Contact Time Microreactors," *Catalysis,* **15**, 98 (2000).

Aghalayam, P., and D. G. Vlachos, "Development of an Analytical Criterion for the Ignition of Premixed Alkane/Air Mixtures Near Platinum Surfaces," *Proc. Eastern States Symp. of Combust. Inst.,* published by the Combustion Institute, Raleigh, NC, p. 217 (1999).

Bodke, A. S., D. A. Olschki, L. D. Schmidt, and E. Ranzi, "High Selectivities to Ethylene by Partial Oxidation of Ethane," *Science,* **285**, 712 (1999).

Boggs, P. T., R. H. Byrd, J. R. Donaldson, and R. B. Schnabel, "ODRPACK-Software for Weighted Orthogonal Distance Regression," *ACM Trans. Math. Softw.,* **15**, 348 (1989).

Box, G. E. P., and N. R. Draper, *Empirical Model-Building and Response Surfaces,* Wiley, New York (1987).

Box, G. E. P., W. G. Hunter, and S. J. Hunter, *Statistics for Experimenters,* Wiley, New York (1978).

Bui, P. A., D. G. Vlachos, and P. R. Westmoreland, "Modeling Ignition of Catalytic Reactors with Detailed Surface Kinetics and Transport: Combustion of H_2/Air Mixtures Over Platinum Surfaces," *Ind. Eng. Chem. Res.,* **36**, 2558 (1997a).

Bui, P. A., E. A. Wilder, D. G. Vlachos, and P. R. Westmoreland, "Hierarchical Reduced Models for Catalytic Combustion: H_2/Air Mixtures near Platinum Surfaces," *Combust. Sci. Technol.,* **129**, 243 (1997b).

Corana, A., M. Marchesi, C. Martini, and S. Ridella, "Minimizing Multimodal Functions of Continuous Variables with the 'Simulated Annealing' Algorithm," *ACM Trans. Math. Softw.,* **13**, 262 (1987).

Deutschmann, O., R. Schmidt, and F. Behrendt, "Interaction of Transport and Chemical Kinetics in Catalytic Combustion of H_2/O_2 Mixtures on Pt," *Proc. Int. Symp. on Transport Phenomena in Combust.,* San Francisco, p. 166 (1995).

Dumesic, I. A., D. F. Rud, L. M. Aparicio, J. E. Rekoske, and A. A. Revino, *The Microkinetics of Heterogeneous Catalysis,* Amer. Chem. Soc. (1993).

Eiteneer, B., C.-L. Yu, M. Goldenberg, and M. Frenklach, "Determination of Rate Coefficients for Reactions of Formaldehyde Pyrolysis and Oxidation in the Gas Phase," *J. Phys. Chem. A,* **102**, 5196 (1998).

Fernandes, N., Y. K. Park, and D. G. Vlachos, "The Autothermal Behavior of Platinum Catalyzed Hydrogen Oxidation: Experiments and Modeling," *Combust. Flame,* **118**, 164 (1999).

Frenklach, M., "Systematic Optimization of a Detailed Kinetic Model Using a Methane Ignition Example," *Combust. Flame,* **58**, 69 (1984).

Frenklach, M., and D. L. Miller, "Statistically Rigorous Parameter Estimation in Dynamic Modeling Using Approximate Empirical Models," *AIChE J.,* **31**, 498 (1985).

Frenklach, M., H. Wang, and M. J. Rabinowitz, "Optimization and Analysis of Large Chemical Kinetic Mechanisms Using the Solution Mapping Method—Combustion of Methane," *Prog. Energy Combust. Sci.,* **18**, 47 (1992).

Goetsch, D. A., and L. D. Schmidt, "Microsecond Catalytic Partial Oxidation of Alkanes," *Science,* **271**, 1560 (1996).

Goffe, W. L., G. D. Ferrier, and J. Rogers, "Global Optimization of Statistical Functions with Simulated Annealing," *J. Econ.,* **60**, 65 (1994).

Helton, J. C., ‘‘Uncertainty and Sensitivity Analysis Techniques for Use in Performance Assessment for Radioactive Waste Disposal,’’ *Reliab. Eng. Syst. Safety,* **42**, 327 (1993).

Hickman, D. A., and L. D. Schmidt, ‘‘Synthesis Gas Formation by Direct Oxidation of Methane over Pt Monoliths,’’ *J. Catal.,* **138**, 267 (1992).

Ikeda, H., J. Sato, and F. A. Williams, ‘‘Surface Kinetics for Catalytic Combustion of Hydrogen-Air Mixtures on Platinum at Atmospheric Pressure in Stagnation Flows,’’ *Surf. Sci.,* **326**, 11 (1995).

Jones, D. R., M. Schonlau, and W. J. Welch, ‘‘Efficient Global Optimization of Expensive Black-Box Functions,’’ *J. Global Optimiz.,* **13**, 455 (1998).

Kalamatianos, S., Y. K. Park, and D. G. Vlachos, ‘‘Two-Parameter Continuation Algorithms for Computing Ignitions and Extinctions: Sensitivity Analysis, Parametric Dependence, Mechanism Reduction, and Stability Criteria,’’ *Combust. Flame,* **112**, 45 (1998).

Lombardo, S. J., and A. T. Bell, ‘‘A Review of Theoretical Models of Adsorption, Diffusion, Desorption, and Reaction of Gases on Metal-Surfaces,’’ *Surf. Sci. Rep.,* **13**, 1 (1991).

Miller, D., and M. Frenklach, ‘‘Sensitivity Analysis and Parameter Estimation in Dynamic Modeling of Chemical Kinetics,’’ *Int. J. Chem. Kinet.,* **15**, 677 (1983).

Myers, R. H., *Response Surface Methodology,* Allyn & Bacon, Boston (1971).

Park, Y. K., P. Aghalayam, and D. G. Vlachos, ‘‘A Generalized Approach for Predicting Coverage-Dependent Reaction Parameters of Complex Surface Reactions: Application to H_2 Oxidation over Platinum,’’ *J. Phys. Chem. A,* **103**, 8101 (1999).

Pfefferle, W. C., and L. D. Pfefferle, ‘‘Catalytically Stabilized Combustion,’’ *Prog. Energy Combust. Sci.,* **12**, 25 (1986).

Prasad, R., L. A. Kennedy, and E. Ruckenstein, ‘‘Catalytic Combustion,’’ *Catal. Rev.−Sci. Eng.,* **26**, 1 (1984).

Rinnemo, M., M. Fassihi, and B. Kasemo, ‘‘The Critical Condition for Catalytic Ignition. H_2/O_2 on Pt,’’ *Chem. Phys. Lett.,* **211**, 60 (1993).

Sacks, J., S. B. Schiller, and W. J. Welch, ‘‘Designs for Computer Experiments,’’ *Technometrics,* **31**, 41 (1989a).

Sacks, J., W. J. Welch, T. J. Mitchell, and H. P. Wynn, ‘‘Design and Analysis of Computer Experiments,’’ *Stat. Sci.,* **4**, 409 (1989b).

Satterfield, C. N., *Heterogeneous Catalysis in Industrial Practice,* 2nd ed., McGraw-Hill, New York (1991).

Sautet, P., and J. Paul, ‘‘Low Temperature Adsorption of Ethylene and Butadiene on Platinum and Palladium Surfaces,’’ *Catal. Lett.,* **9**, 245 (1991).

Shustorovich, E., ‘‘Bond-Order Conservation Approach to Chemisorption and Heterogeneous Catalysis: Applications and Implications,’’ *Adv. Catal.,* **37**, 101 (1990).

Shustorovich, E., and H. Sellers, ‘‘The UBI-QEP Method: A Practical Theoretical Approach to Understanding Chemistry on Transition Metal Surfaces,’’ *Surf. Sci. Rep.,* **31**, 1 (1998).

Thiel, P. A., and T. E. Madey, ‘‘The Interaction of Water with Solid Surfaces: Fundamental Aspects,’’ *Surf. Sci. Rep.,* **7**, 211 (1987).

Tomlin, A. S., T. Turanyi, and M. J. Pilling, ‘‘Mathematical Tools for the Construction, Investigation, and Reduction of Combustion Mechanisms,’’ *Elsevier Sci. J.,* **35**, 293 (1997).

Trevino, C., ‘‘Analysis for the Catalytic Ignition of Methane in a Stagnation-Point Flow,’’ *AIChE J.,* **45**, 567 (1999).

Van Santen, R. A., *Theoretical Heterogeneous Catalysis,* World Scientific, Singapore (1991).

Van Santen, R. A., and M. Neurock, ‘‘Theory of Surface-Chemical Reactivity,’’ *Handbook of Heterogeneous Catalysis,* G. Ertl, H. Knozinger, and J. Weitkamp, eds., VCH, Weinheim, p. 991 (1997).

Wahnström, T., E. Fridell, S. Ljungström, B. Hellsing, B. Kasemo, and A. Rosén, ‘‘Determination of the Activation Energy for OH Desorption in the $H_2 + O_2$ Reaction on Polycrystalline Platinum,’’ *Surf. Sci. Lett.,* **223**, L905 (1989).

Williams, W. R., C. M. Marks, and L. D. Schmidt, ‘‘Steps in the Reaction $H_2 + O_2 = H_2O$ on Pt: OH Desorption at High Temperatures,’’ *J. Phys. Chem.,* **96**, 5922 (1992).

Yetter, R. A., H. Rabitz, and R. M. Hedges, ‘‘A Combined Stability-Sensitivity Analysis of Weak and Strong Reactions of Hydrogen/Oxygen Mixtures,’’ *Int. J. Chem. Kinet.,* **23**, 251 (1991).

Manuscript received Jan. 14, 2000, and revision received Apr. 27, 2000.